20th Annual Conference of the Canadian Nuclear Society
Montreal, Quebec, Canada / May 30 - June 2, 1999

Commercial Aircrew Radiation Dosimetry using a Tissue Equivalent Proportional Counter

A.R. Green, B.J. Lewis, LG.I. Bennett and M. Pierre
Royal Military College of Canada, P.O. Box 17000 Stn Forces, Kingston, Ontario, Canada K7K 7B4

T. Cousins
Defence Research Establishment Ottawa, Ottawa, Ontario, Canada K1A 0Z4

Abstract

As part of a continuing study on the occupational exposure of Canadian-based aircrew, a Tissue Equivalent Proportional Counter (TEPC) was used to monitor this exposure on representative Canadian-based flight routes. The microdosimetric data obtained from these flights were compared to that obtained from several terrestrial sources and were used to characterize the radiation field at jet altitudes. The data showed that there is a hardening of the radiation field at latitudes close to the geomagnetic pole. In addition, the accuracy of the TEPC data was confirmed by a comparison to data from other conventional detectors.

1 Introduction

The International Commission on Radiological Protection (ICRP) recently recommended that in-flight natural background exposure of aircrew should be considered an occupational exposure.[1] This paper describes the use of a TEPC to estimate this exposure from several Canadian-based commercial flights. After proper calibration, a TEPC can provide not only an indication of radiation levels, but also the microdosimetric distribution of the radiation as a function of lineal energy. Thus the TEPC plays an important role in the measurement and characterization of this complex radiation field.

The radiation environment at jet altitudes (9 to 19 km in altitude) consists mainly of the secondary radiation (e.g., neutrons, protons, gamma rays, muons and pions) produced when galactic cosmic rays interact with the oxygen and nitrogen nuclei of the air in the upper layer of the atmosphere.[2] The intensity and composition of this radiation field vary with geomagnetic latitude due to the increased deflection of the primary galactic cosmic rays by the Earth's magnetic field near the equator. The complexity of this mixed radiation field presents certain challenges (which are not present in typical terrestrial applications) when measuring dosimetric quantities. The TEPC is the only instrument that is capable of measuring the total dose equivalent in a complex radiation field such as that experienced at jet altitudes.

2 Experimental

Microdosimetric spectra were obtained with a TEPC from several types of terrestrial radiation fields and from the cosmic radiation field on board several commercial flights originating from Canada. The TEPC, described in detail below, was designed by Battelle, Pacific Norwest National Laboratories to be completely portable. It is battery-powered and all of its components are fitted inside an aluminum case that can be taken into the aircraft cabin as carry-on luggage. Battelle proprietary software was used to download the stored data and to convert the raw binary data to spectral results that were stored as text files. Additional Battelle proprietary software provided absorbed dose (D) and dose equivalent (H) values,

and further analysis yielded the microdosimetric quantities of frequency-mean lineal energy ($\bar{y}_F$), dose-mean lineal energy ($\bar{y}_D$) and average quality factor ($\overline{Q}$), as described in the next section. Essentially, the output is a microdosimetric dose distribution that reveals the relative penetrating capability of the components of a complex radiation field. The spectrum is similar to a pulse-height spectrum produced by a multichannel analyzer (MCA) in gamma-ray spectroscopy, except that, instead of sorting the detected radiation according to emitted energy, the radiation is sorted according to the energy imparted to the absorbing material.

On two separate series of flights, the response of the TEPC at jet altitudes was compared to that from a suite of conventional instruments that provided separate measurements of the non-neutron (low-LET) and neutron (high-LET) components of the radiation field. On a 1997 First Air scientific flight, aluminum oxide thermoluminescent detectors (TLDs) and an Eberline FHT 191 N ionization chamber were used to measure the non-neutron component of the field, while a modified (lead-covered) Eberline NRD (Andersson-Braun) type rem-meter (LCRM) and Bubble Technology Industries, Inc. neutron bubble detectors were used for measurement of the neutron radiation component. On a subsequent 1998 British Airways flight, the TEPC response was compared to that from a series of passive detectors only (non-neutron-sensitive TLDs, and neutron-sensitive bubble detectors and track-etch detectors).

2.1 Technical Description of the TEPC

The Battelle TEPC consists of a grounded anode type spherical walled detector with an attached preamplifier, a spectrometer box that stores full data spectra each minute on a non-volatile flash memory card and a battery box containing 16 standard 'D' cells. In general, a TEPC allows experimental determination of the microscopic distribution of energy deposition in irradiated matter by using a large low-density cavity to simulate a microscopic volume of tissue of equivalent atomic composition.[3] In the Battelle TEPC, the detector cavity (Far West Technology LET-SW-5) is designed to emulate a 2 ≥m-diameter spherical tissue site. It consists of a 12.70-cm (5")-diameter hollow sphere with walls made of 2.13-mm thick A-150 tissue equivalent plastic. This sphere is filled with 7 torr of pure propane as a tissue equivalent gas. The large detector provides a large cross-sectional area, which enables a rapid collection of a statistically significant sample in a low flux area such as that on board an aircraft. A 0.07 mm-diameter stainless steel collecting wire is stretched across the diameter of the sphere in order to detect the electrical signal that results from the ionization of the detector gas following an energy-deposition event. The pulse size of this signal is directly proportional to the number of ion pairs formed (and hence proportional to the energy imparted) and is linearly amplified in magnitude by gas multiplication. Because the dynamic range of these pulses is often very large (e.g., over 5 orders of magnitude for fast neutrons), the spectrum of energy imparted is measured in two different sections, differing in gas gain level, and hence in resolution, from each other.[3] In each region, the signals received from the detector are sorted by a MCA into 256 channels according to pulse height (which can then be correlated to energy imparted).

2.2 Data Analysis

The principal quantities used for microdosimetric purposes are energy imparted (≈) and other stochastic quantities related to energy imparted, such as lineal energy (y), and the expectation values of these quantities.[3] The lineal energy (usually given in units of keV/≥m) is the quotient of the energy

imparted to the irradiated matter in a given volume by a single energy-deposition event to the mean chord length:[3]

$$y = \frac{\varepsilon}{\bar{\ell}} \tag{1}$$

where, for a convex site with a volume V and surface area S, the mean chord length can be calculated from Cauchy's theorem:[4]

$$\bar{\ell} = \frac{4V}{S}. \tag{2}$$

The output of the Battelle TEPC proprietary software provides the number of counts (n) in each of the 256 channels in the two different gain regions. In the high-gain region, the 256 channels each have a bin width of 0.1 keV/≥m to cover the lineal energy spectrum from 0 to 25 keV/≥m, i.e., for low-lineal energy radiation, such as gamma rays. In the low-gain region, which covers up to 1275 keV/≥m (i.e. for high-lineal energy radiation, such as neutrons), the bins each have a width of 5 keV/≥m. The lineal energy for a given channel (y_i) is calculated as the mid-point lineal energy of the channel. The two overlapping segments are joined such that the integral count up to a given value of y is equal in both the high-gain and low-gain segments. Due to the electronic noise level, it is not possible to measure the number of counts accurately in the first four channels of the high-gain region. To account for this deficiency, an extrapolation to zero lineal energy is made so that the $yn(y)$ values in each of these channels is set equal to the maximum recorded value of $yn(y)$ (usually found in the fifth channel). The resulting complete spectrum represents a frequency distribution of event sizes.

A detailed description of the treatment of this frequency distribution is given in Reference 5; however, the relevant equations are summarized below. In order to compare spectra measured under different conditions, it is necessary to normalize the frequency distribution so that the total area under the curve represents one event.[6] This can be accomplished by utilizing the probability density function $f(y)$ (also called the lineal energy distribution), which is defined as

$$f(y) = \frac{dF(y)}{dy} \approx \frac{\Delta F(y_i)}{\Delta y_i} \equiv f(y_i) = \frac{n(y_i)}{\Delta y_i \sum_{i=0}^{\infty} n(y_i)}, \tag{3}$$

where $F(y)$ is the probability that the lineal energy is equal to or less than y and Δy_i is the appropriate bin width as described above.[3] Note that this function satisfies the normalization condition of any probability density function, i.e.,

$$\int_0^{\infty} f(y)dy = 1. \tag{4}$$

The frequency-mean lineal energy, $\bar{y}_F$, is the expectation value of y (i.e., the average of the observed values of y), as weighted by the frequency probability density. From standard calculus theory:

$$\bar{y}_F = \frac{\int_0^{\infty} yf(y)dy}{\int_0^{\infty} f(y)dy} = \int_0^{\infty} yf(y)dy \approx \sum_{i=0}^{\infty} y_i f(y_i)\Delta y_i = \frac{\sum_{i=0}^{\infty} y_i n(y_i)}{\sum_{i=0}^{\infty} n(y_i)}. \tag{5}$$

The second relation in Equation (5) follows from the normalization of Equation (4) and the last relation follows from Equation (3).

It is often more useful to consider the dose distribution of y (as opposed to the frequency distribution). If $D(y)$ is the fraction of absorbed dose delivered with lineal energy less than or equal to y, then the dose probability density, $d(y)$, is defined as:[3]

$$d(y) \equiv \frac{dD(y)}{dy}. \tag{6}$$

The relationship between $d(y)$, $f(y)$ and $\bar{y}_F$ is given by:[3]

$$d(y) \equiv \frac{1}{\bar{y}_F} y f(y). \tag{7}$$

Note that $d(y)$ also has the normalization property expected from a probability density function (as described by Equation (4)). Analogous to $\bar{y}_F$, the dose-mean lineal energy, $\bar{y}_D$, is an expectation value of y weighted with the dose probability density, i.e.,

$$\bar{y}_D \equiv \int_0^\infty y d(y) dy. \tag{8}$$

Since the values both y and $d(y)$ can range over several orders of magnitude, a linear representation will not show the details of the distribution.[4] For this reason, the dose distribution is normally plotted in a semi-logarithmic representation as $yd(y)$ versus $\log y$. The normalization property of $d(y)$ remains unchanged in this representation since

$$\int_0^\infty d(y) dy \equiv \int_0^\infty y d(y) \left(\frac{1}{y \ln y}\right) \equiv 2.303 \int_0^\infty y d(y) \left(\frac{1}{y \log y}\right) \equiv 1. \tag{9}$$

From Equation (9), one can also see that the area under the curve in a given y interval is proportional to the fraction of *dose* delivered by events with lineal energies in this interval.

Similarly, a *dose equivalent* probability density function can be calculated using $h(y)=d(y)q(y)$, where $q(y)$ is the quality factor relationship taken from the ICRU Publication 40.[7] Alternatively, $q(y)$ can be replaced by the Q(LET) relationship given in ICRP-60 so that $h(y)=d(y)Q(LET)$. Substituting the ICRU-40 $q(y)$ by the ICRP-60 Q(LET) relationship results in only a 3% decrease in the integrated dose equivalent and has been adopted for the present analysis.[5]

As previously discussed, the TEPC is used to simulate a microscopic volume of tissue. In order to apply the simulation principle, it is required that the energy loss of passing charged particles is identical in the tissue sphere and the gas sphere for equivalent trajectories. Thus, for a tissue sphere of diameter d_t and a gas detector sphere of diameter d_d,

$$\Delta E_t \equiv (S/\rho)_t \rho_t d_t \equiv (S/\rho)_d \rho_d d_d \equiv \Delta E_d \tag{10}$$

where ΔE_t and ΔE_d are the mean energy losses from the charged particle in tissue (t) and gas detector (d), $(S/\rho)_t$ and $(S/\rho)_d$ are the mass stopping powers, and ρ_t and ρ_d are the densities. If the atomic composition of the tissue and gas are identical, and the mass stopping powers are independent of density, it follows that

this simulation can be achieved by simply arranging the gas pressure in the low-density gas cavity of the TEPC so that

$$\rho_d d_d \approx \rho_t d_t . \tag{11}$$

This simulation results in an absorbed dose, D, which is equivalent in both the detector and tissue site. Following the derivation procedure described in Reference 5, D (in Gy) is given by

$$D \approx \frac{0.204}{d_d^2} \int_{i\approx 0}^{\infty} y_i n(y_i) \tag{12}$$

where, for the current detector, $d_d = 1.27 \times 10^5$ ≥m. Similarly, the dose equivalent (in Sv) is given by

$$H \approx \frac{0.204}{d_d^2} \int_{i\approx 0}^{\infty} q(y_i) y_i n(y_i) \tag{13}$$

where $q(y)$ is the quality factor. (As mentioned above, *q(y)* has been replaced by the Q(LET) relationship recommended in ICRP-60 for the present analysis.) Both Equations (12) and (13) have been proposed in Reference 8. The average quality factor is further given by:

$$\overline{Q} \approx \frac{H}{D} \approx \int_0^{\infty} q(y) d(y) dy. \tag{14}$$

2.3 Calibration Procedure

Equations (12) and (13) are only strictly applicable to an ideal detector. To account for non-spherical and field edge effects, a given detector must be calibrated so that a correction factor can be applied:

$$D_{real} \approx \xi\, D_{ideal} \text{ and } H_{real} \approx \xi\, H_{ideal} \tag{15a and 15b}$$

Calibration of the TEPC is carried out using a radiation source that produces a known energy deposition in the detector cavity. In this particular case, the initial calibration of the TEPC was conducted by the manufacturer at the Pacific Northwest National Laboratories calibration facility. The detector was exposed to calibrated ^{137}Cs and ^{252}Cf sources at a given distance. The measured absorbed dose rate was compared to that expected for a given source accounting for neutron scattering in air, backscattering and non-uniformity effects. From these measurements, it was determined that ♦ in Equations (15a) and (15b) should be 1.00 for this specific detector.

For routine calibration checks, the detector is equipped with an internal ^{244}Cm source, which, in normal operation, is shielded from the detector cavity by a magnetic shutter. This source emits ~5 MeV alpha particles without emitting any gamma rays.[3] It is possible to accurately determine the theoretical amount of energy imparted, ≈, to the counter gas by these particles. Although the use of range-energy relationships would be more accurate than the use of a stopping power value, ≈ can be determined as a first approximation from the relation

$$\varepsilon \approx (S/\rho)\rho_t d_t \tag{16}$$

which follows from Equation (10). Based on a mass collision stopping power, (S/ρ) = 913 MeV cm^2 g^{-1} for 5.0 MeV alpha particles by tissue-equivalent propane gas[3], a tissue site density, ρ_t = 1 g/cm^3 and a tissue sphere diameter, d_t = 2 ≥m, the energy imparted by a 5 MeV alpha particle in the current detector

cavity is 183 keV. Using Equations (1) and (2), the latter of which reduces to $\bar{l} = d_t/1.5$ for a sphere, this corresponds to a lineal energy of 137 keV/≥m since

$$y \approx 1.5\left(\frac{\varepsilon}{d_t}\right)^{*}. \qquad (17)$$

The actual spectrum (Figure 1) consists of a single Gaussian-shaped peak with a maximum near 152.5 keV/≥m. (This position is slightly different than the position predicted above since the alpha particles are not precisely 5 MeV and range-energy relationships were not used in the prediction.) Note also that due to fluctuations in the energy loss as a result of straggling[3], the peak is broadened slightly such that FWHM (full width at half maximum) is approximately 20 keV/≥m. The position of this peak, which corresponds to channel 30 in the low gain region, is checked before and after each microdosimetric measurement. A second, more sensitive check of the gain shift is made by comparing the absorbed dose rate from the alpha source to previous values.

Coincidentally, the position of this peak corresponds to that of the so-called "proton edge" that appears in all fast neutron microdosimetric spectra. Neutrons impart energy to tissue primarily via recoil protons of energies less than or equal to the neutron energy. In tissue, the maximum LET of protons is near 95 keV/≥m,[4] which means that the maximum energy, ≈, that any proton can deposit in a 2-≥m diameter sphere is 190 keV. Using Equation (17), this ≈ corresponds to a lineal energy of 142.5 keV/≥m. Consequently, the *yd(y)* spectrum for fast neutrons (of energy in excess of 100 keV) exhibits a sharp drop at this lineal energy. The position of this drop, termed the proton edge, can be used as a further means of calibration of the TEPC.[6]

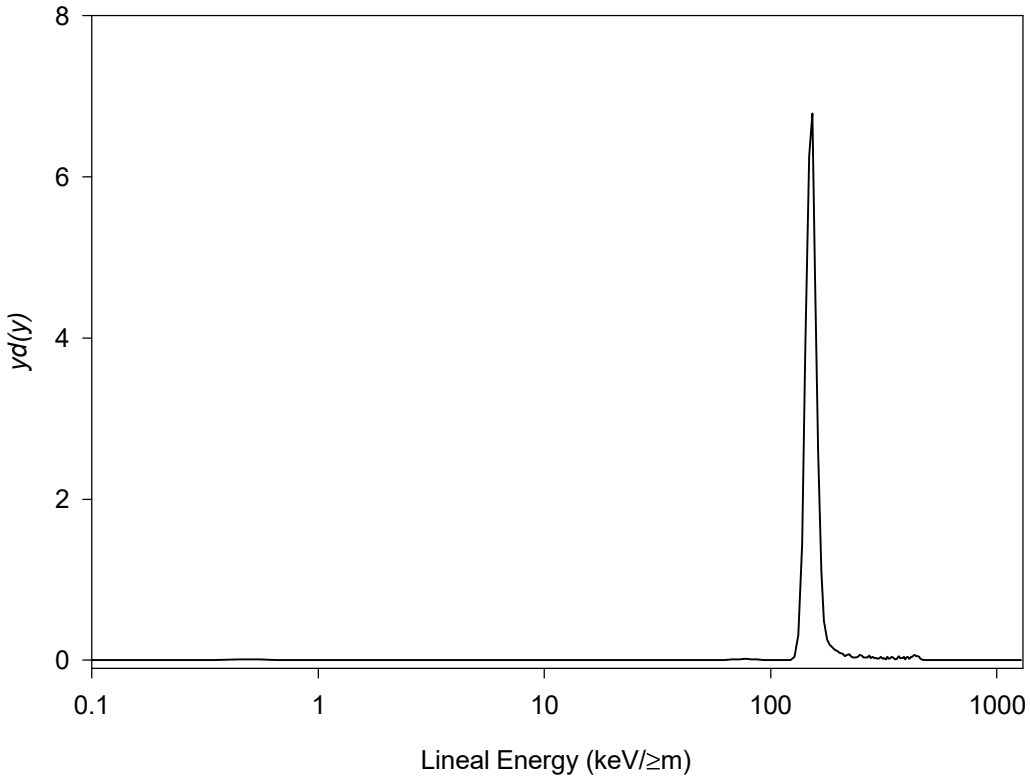

Figure 1. Microdosimetric dose distribution (summed over 1 hour) of internal ^{244}Cm alpha source.

3 Results and Discussion

Since the TEPC can provide not only an indication of radiation levels in a complex (mixed) radiation field, but also the microdosimetric distribution of the radiation, this instrument has found wide application in radiation chemistry, radiobiology, radiation therapy and radiation protection.[4,8,9] For example, TEPCs have been used for radiation protection metrology within Canada on the top deck plate of the NRU (National Research Universal) reactor at AECL's Chalk River Laboratories[10] and at CANDU power plants.[11] The increased demand for reliable dosimetric data with which to assess the exposure of aircrew to cosmic radiation has resulted in the use of TEPCs in several in-flight cosmic radiation measurement campaigns worldwide.[5,12,13,14,15,16] As part of a continuing assessment of the cosmic radiation exposure of Canadian aircrew, the TEPC has been used to take dosimetric measurements on board several Canadian-based commercial flights.

Before taking these in-flight dosimetric measurements, the operation of the TEPC was verified using several common radioisotopic sources, such as ^{137}Cs, ^{60}Co, ^{252}Cf, ^{241}Am-^{9}Be and ^{239}Pu-^{9}Be sources. The individual microdosimetric spectra recorded by the TEPC in each of these fields represent the different constituents present in the radiation field at high altitudes (i.e., the gamma and neutron components of the field). The values of $\bar{y}_F$, $\bar{y}_D$ and $\overline{Q}$ that were obtained from some of these sources are shown in Table 1. These quantities were determined using Equations (5), (8) and (14), respectively. The quantity $\bar{y}_F$ gives the average lineal energy per event; however, the quantities $\bar{y}_D$ and $\overline{Q}$ are more useful in radiation protection since they are, to a first approximation, proportional to the relative biological effectiveness (RBE) of the measured radiation.[4] In particular, $\overline{Q}$ should provide an approximation of the radiation weighting factor, w_R, as defined in ICRP-60.[1] For instance, the experimental $\overline{Q}$ value of 24 obtained for alpha particles from the data in Figure 1 agrees quite well with the w_R value of 20 recommended in ICRP-60 for alpha particles. The values obtained from a gamma ray spectrum and from a mixed neutron-gamma ray spectrum are discussed below.

The *yd(y)* plot recorded by the TEPC following exposure to a ^{137}Cs source is shown in Figure 2. This dose distribution is typical of that obtained in a gamma ray field. In this case, the spectrum arises from the deposition of energy by the secondary electrons that are produced by the interaction of the gamma rays with the tissue equivalent wall or gas.[6] The maximum deposition of energy takes place when the range of the electrons matches that of the cavity size, which results in the formation of an edge or shoulder.[6] As seen in Figure 2, this edge occurs close to 10 keV/≥m for a cavity with a simulated diameter of 2 ≥m. For this reason, the Battelle proprietary TEPC software classifies any radiation with a lineal energy below 10 keV/≥m as "gamma" radiation. Note that the dashed line in this figure represents an extrapolation of the actual data to zero lineal energy. The choice of extrapolation method contributes to uncertainties in the calculations of $\bar{y}_F$ and absorbed dose. Since the dosimetric distribution obtained from a gamma ray source falls completely below 10 keV/≥m, these uncertainties will be most pronounced for gamma ray fields. The value of $\overline{Q}$ calculated from the data in this figure is 1.1. This value is slightly higher than the expected value of 1 for gamma rays due to the contribution of a very few counts at lineal energies greater than 10 keV/≥m. (i.e., a very few counts in the high-lineal energy bins are amplified by a Q(LET) value which is greater than 1.) Other groups have also reported values of $\overline{Q}$ slightly greatly than 1 from TEPC measurements in a gamma ray field.[17]

Table 1 Microdosimetric Quantities obtained from Terrestrial Sources

Source	Type of Radiation	$\bar{y}_F$ (keV/≥m)[a]	$\bar{y}_D$ (keV/≥m)	$\bar{Q}$
^{137}Cs	≠rays	0.36 o 0.13	7.2 o 0.8	1.1 o 0.2
^{239}Pu-^{9}Be	neutrons, ≠rays	1.39	51 o 6	9 o 2
^{244}Cm	↵ particles	14.0	150 o 20	24 o 4

[a]The maximum error on $\bar{y}_F$ is 35%, most of which is associated with the extrapolation to zero lineal energy; thus, this error will be most significant for gamma ray spectra.

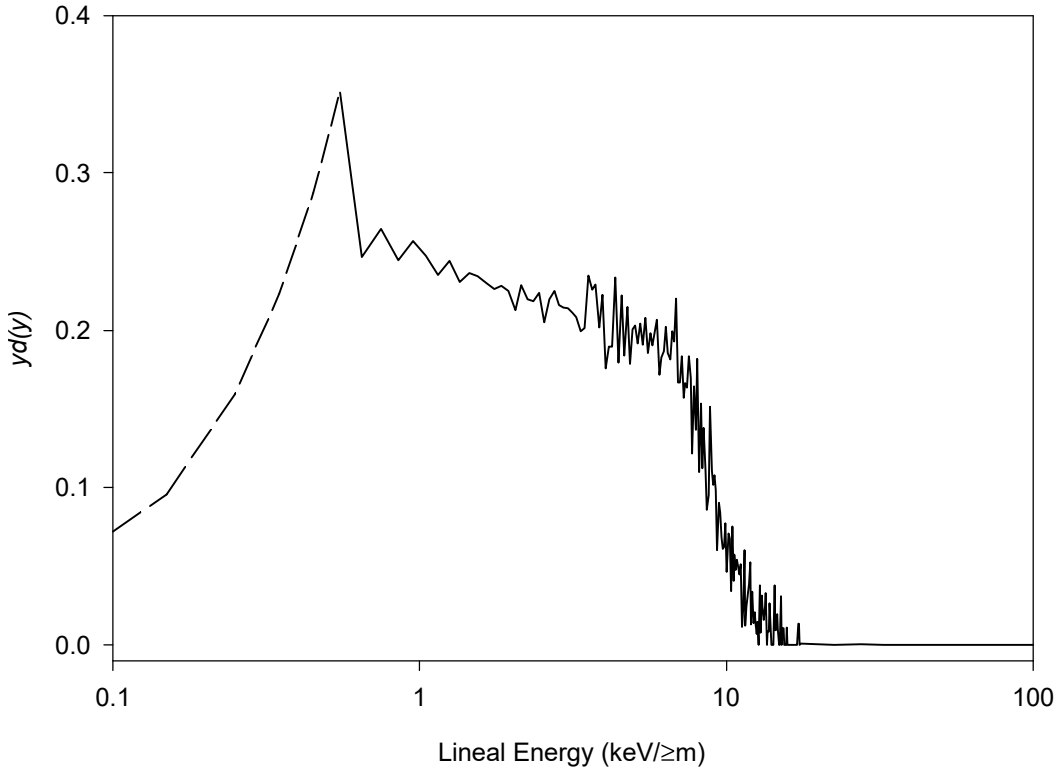

Figure 2. Microdosimetric dose distribution (summed over 1 hour) from a ^{137}Cs ≠ray source.

Figure 3 shows a typical dose distribution obtained from a mixed neutron and gamma radiation field, in particular the ^{239}Pu-^{9}Be source at the Defence Research Establishment in Ottawa (DREO). In this case, decay of the ^{239}Pu produces alpha particles that in turn interact with the ^{9}Be to produce neutrons via (↵,n) reactions. The neutrons are emitted in the form of an energy spectrum with two significant peaks at 5.0 MeV and 7.5 MeV and three smaller peaks at 3.0, 6.5 and 9.8 MeV,[18] with an average neutron energy of 4.6 MeV.[19] This production of neutrons is accompanied by gamma ray emission, which contributes roughly 1/3 of the total absorbed dose (i.e., the area under the curve from 0 to 10 keV/≥m in Figure 3 is about 1/3 the total area). The more obvious feature of the spectrum in Figure 3 is the proton peak between 10 and 150 keV/≥m. As described in Section 2.3, the sharp cut-off near 150 keV/≥m is the "proton edge" which appears in all fast neutron spectra. Above the proton edge, there is another small peak that

represents about 5% of the total area. This peak is generated by events due to alpha particles produced in (n,↵) reactions.[6] Similar to a proton edge, an "alpha edge" exists near 360 keV/≥m, which represents the maximum event size from an alpha particle.[6] Beyond this alpha edge, events due to heavy recoil ions of carbon, nitrogen and oxygen are recorded.[6] The proton peak is further emphasized by displaying the same data in a dose equivalent distribution (Figure 4). As described in Section 2.2, in this representation, the values of *d(y)* are multiplied by the ICRP-60-recommended *Q*(LET) values. According to this ICRP-60 *Q*(LET) relationship, the value of *Q* is at a maximum for particles with an LET of 100 keV/≥m, which results in the sharp peak seen at 100 keV/≥m in Figure 4. The area under this proton peak (i.e., between 10 and 160 keV/≥m) represents 87% of the total area and hence 87% of the total dose equivalent. A $\overline{Q}$ value of 9 was calculated from these data for the entire ^{239}Pu-^{9}Be spectrum. Using the values of dose equivalent (*H*) and absorbed (*D*) calculated for the portion of the spectrum above 10 keV/≥m, a $\overline{Q}$ value of 12.7 is obtained for the "non-gamma" component. This compares quite well with a w_R value of 12.5 calculated for a neutron energy (E_n) of 4.6 MeV, using the ICRP-60-recommended relationship:[1]

$$w_R(E_n) = 5 + 17\exp\left[\frac{-(\ln 2E_n)^2}{6}\right] \qquad (18)$$

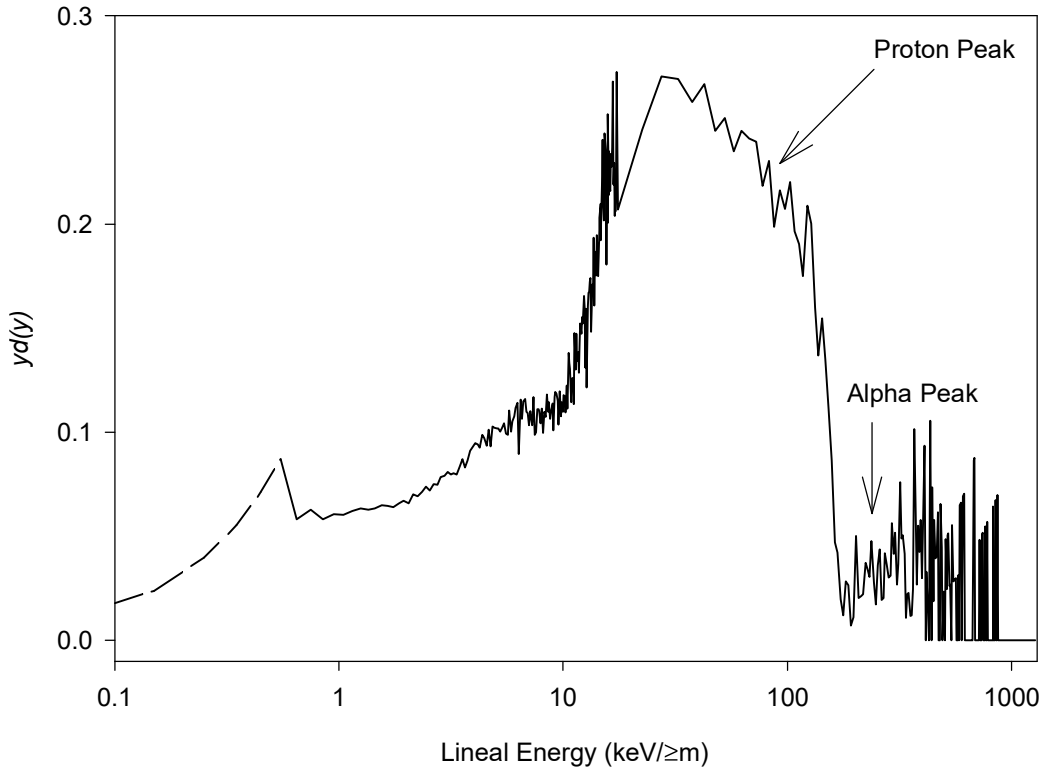

Figure 3. Microdosimetric dose distribution (over 226 minutes) from a ^{239}Pu-^{9}Be neutron source.

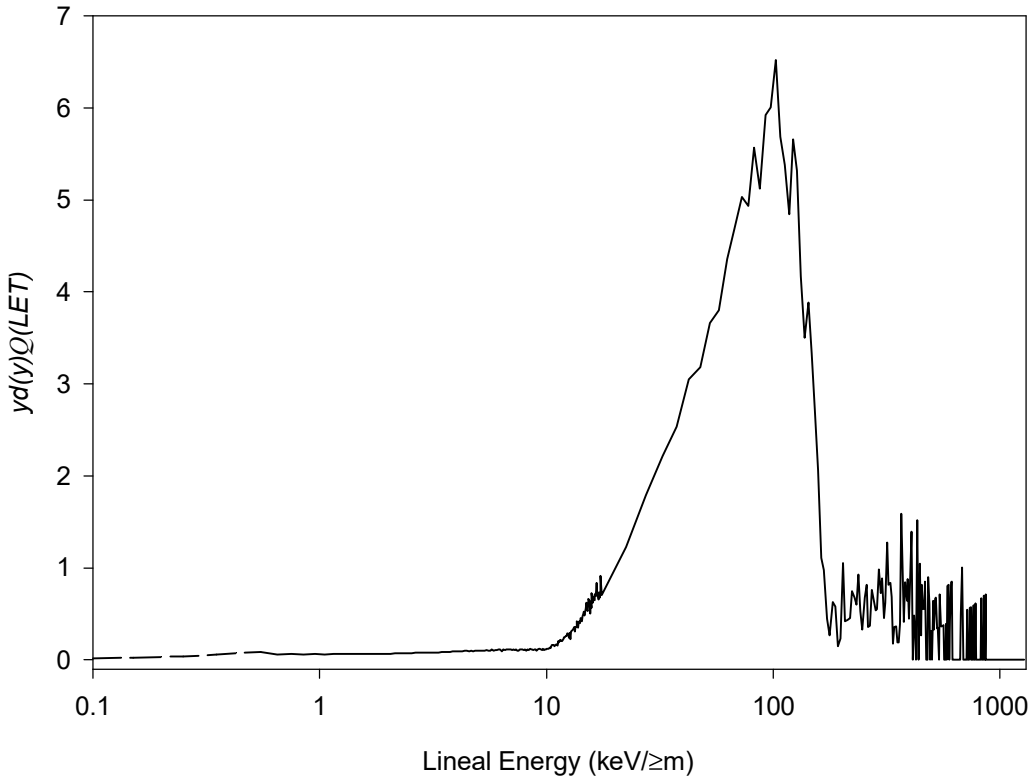

Figure 4. Dose equivalent distribution of the data displayed in Figure 3 from a ^{239}Pu-^{9}Be source.

The individual microdosimetric spectra recorded by the TEPC in these terrestrial fields provide an indication of the different constituents present in the radiation field at jet altitudes (i.e., the non-neutron and neutron components of the field). Actual jet altitude microdosimetric spectra were obtained with the TEPC at altitudes between 8.5 and 12.5 km (28 000 - 41 000 feet) on board several commercial flights originating from Canada. A summary of the routes covered and values of $\bar{y}_F$, $\bar{y}_D$ and $\bar{Q}$ for four global flight regions are shown in Table 2. In all cases, the $\bar{Q}$ values are greater than 1 and the $\bar{y}_D$ values are greater than 10 keV/≥m, which indicates a significant high-LET (>10 keV/≥m) contribution to the radiation field.

The proportion of the cosmic radiation field that arises from neutrons changes as a function of latitude. Specifically, the neutron fraction is highest at latitudes above the geomagnetic knee, which occurs at a geomagnetic latitude of approximately 60πN, and lowest in equatorial regions.[2] This increase in the neutron fraction should result in higher values of both $\bar{y}_D$ and $\bar{Q}$ for the more northerly routes. The data summarized in Table 2 show that this is indeed the case. For a flight route within northern Canada that lies entirely above the position of the geomagnetic knee (Ottawa to Iqaluit, Iqaluit to Resolute Bay, Resolute Bay to Nanisivik, Nanisivik to Iqaluit, Iqaluit to Ottawa), $\bar{y}_D$ is 23 keV/≥m and $\bar{Q}$ is 3.4. These values are significantly higher than those measured in the current study on trans-Canada, trans-Atlantic and trans-Pacific flight routes that are either partially or completely below the geomagnetic knee ($\bar{y}_D$=15 keV/≥m and $\bar{Q}$=2.3). $\bar{Q}$ values between 2.1 and 2.4 have also been reported in the literature from TEPC measurements on board flights from Buenos Aires to Paris, from Tokyo to Paris and between the Swedish cities of Stockholm and Umea.[12,13]

Table 2 Microdosimetric Quantities Measured on Canadian-based Flights

Global Flight Region	Routes Covered[a]	$\bar{y}_F$ (keV/≥m)	$\bar{y}_D$ (keV/≥m)	$\bar{Q}$
Trans-Atlantic	YYZ-LHR (return) YYZ-FRA (return) YUL-LHR LHR-YVR	0.358	14 o 2	2.3 o 0.4
Trans-Canada	YYZ-YVR (2) YVR-YYZ (3)	0.359	15 o 2	2.3 o 0.4
Northern Canada	YOW-YFB-YRB- YSR-YFB-YOW	0.541	23 o 3	3.4 o 0.6
Trans-Pacific	YVR-KIX KIX-YVR	0.334	15 o 2	2.2 o 0.4

[a]Airport codes are YYZ-Toronto International; LHR-Heathrow, London, UK; FRA-Frankfurt, Germany; YUL-Dorval, Montreal; YVR-Vancouver; YOW-Ottawa; YFB-Iqaluit; YRB-Resolute Bay; YSR-Nanisivik; KIX-Osaka, Japan

The hardening of the spectrum at more northerly latitudes is also evident from the dose distributions displayed in Figure 5 for a flight from Toronto to London (UK) with British Airways and for a round trip flight, following the path described above, within northern Canada on First Air. In both cases, most of the absorbed dose distribution is observed below 10 keV/≥m; however, the area under the proton peak (10-160 keV/≥m) is about twice as large for the spectrum obtained in northern Canada (20% versus 10% for the YYZ-LHR spectrum). In the dose equivalent distribution (not shown), the area under the proton peak represents 49% of the total dose equivalent received on the YYZ-LHR flight and 64% of the total dose equivalent received on the northern flights. In both cases, the area under the alpha peak is about 1% of the total absorbed dose distribution. In addition, although the data is scattered due to poor counting statistics, about 1% of the total absorbed dose arises from particles with a high lineal energy (> 360 keV/≥m). (The statistical noise in this region is further enhanced by the multiplication of a low number of counts by a large value of y. For instance a single count at 800 keV/≥m produces a $yd(y)$ value which is equivalent to that produced by 120 counts at 10 keV/≥m.) These high-lineal energy particles include fragmentation products produced by the interaction of atmospheric nuclei with the primary high-energy protons, as well as some of the primary galactic particles and so-called HZE particles. Although they contribute a small amount to the absorbed dose, they can induce significant biological damage.[2]

In order to verify the response of the TEPC, conventional dosimeters were also used on the First Air flights within northern Canada and on the British Airways Toronto to London (return) flights. As described in Section 2, TLDs, an ionization chamber (IC), a LCRM and bubble detectors (BD) were used on the First Air flight and TLDs, bubble detectors and track-etch detectors were used on the British Airways flights. The dose equivalent, as measured by this equipment, for the non-neutron and neutron components is compared to the total dose equivalent measurement by the TEPC in Table 3. These independent detectors confirmed that the total dose equivalent estimated by the TEPC is equivalent to the sum of the non-neutron (TLD or IC) measurement and the neutron (BD, LCRM or track-etch detector) measurement.

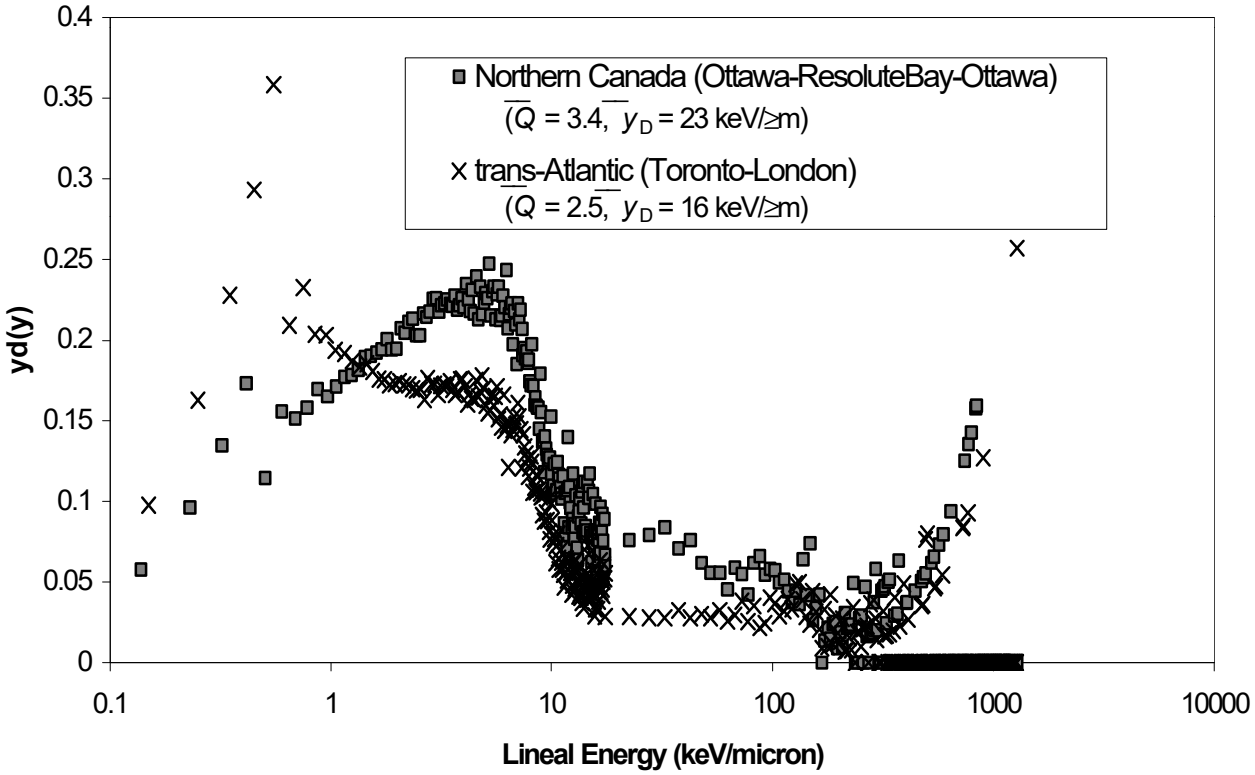

Figure 5. Comparison of microdosimetric data for two Canadian-based routes[5]

Table 3 Comparison of Dose Equivalent Measurements from Various Instruments

Flight Route	Total Dose Equivalent (≥Sv)	Non-Neutron Dose Equivalent[a] (≥Sv)		Neutron Dose Equivalent (≥Sv)		
	TEPC	TLD	IC	BD	LCRM	Track-Etch
YOW-YFB-YRB-YSR-YFB-YOW[b]	54 o 28	26 o 3	22 o 1	29 o 11	31 o 6	N/A
YYZ-LHR-YYZ	82 o 12	48 o 4	N/A	33 o 6	N/A	28 o 13[c]

[a]Calculated assuming an 18% contribution by protons (with w_R=5) to the non-neutron component[5]
[b]Data from Reference 5
[c]Track-etch detectors and data were provided by the National Radiological Protection Board, UK

4 Conclusion

The TEPC is an important tool in the monitoring of aircrew radiation exposure. It can provide not only the total dose equivalent in a complex mixed radiation field, but also information on the quality of the radiation. The data obtained by the TEPC confirmed that aircrew are exposed to radiation that is more penetrating than that typically experienced by terrestrial radiation workers. In addition, there is a hardening of this radiation field at high latitudes as a result of the decreased ability of the Earth's magnetic field to deflect incoming particles at higher latitudes. The accuracy of the total dose equivalent estimate provided by the TEPC was verified using various independent passive and active dosimeters.

Acknowledgements

The authors would like to thank H. Goldberg of the Air Transport Association of Canada (ATAC), C. Thorp of the Director General Nuclear Safety (DGNS) of the Department of National Defence and J. Servant of Transport Canada for their assistance in the study. The authors would also like to express their gratitude to J. Lafrance of First Air, D. Irvine of British Airways and J. Nakielny of Air Canada, and the management of these airlines, for flight arrangements. Finally, the authors would like to thank L. Hager and D. Bartlett of NRPB for the use of their passive dosimeter boxes and for the analysis of the results; T. Jones, J.R. Brisson and B. Hoffarth of DREO for their assistance with the ^{239}Pu-^{9}Be measurements and with the in-flight measurements; and L. Braby of Texas A & M University and T. Conroy of Battelle, Pacific Northwest Laboratories for discussions on TEPC measurement and analysis. Financial support for this study was received from ATAC, DGNS and Transport Canada.

References

1. International Commission on Radiological Protection, "1990 Recommendations of the International Commission on Radiological Protection," ICRP Publication 60, Pergamon Press, Oxford (1991).

2. G. Reitz, "Radiation Environment in the Stratosphere," Radiat. Prot. Dosim., **48**, (1993) 5-20.

3. International Commission on Radiation Units and Measurements, "Microdosimetry," ICRU Report 36, December 1983.

4. H.H. Rossi and M. Zaider, Microdosimetry and Its Applications, Springer-Verlag, New York (1996).

5. B.J. Lewis, P. Tume, L.G.I. Bennett, M. Pierre, A.R. Green, T. Cousins, B.E. Hoffarth, T.A. Jones, J.R. Brissson, "Cosmic Radiation Exposure on Canadian-Based Commercial Airline Routes," submitted to Radiat. Prot. Dosim. (1999).

6. A.J. Waker, "Principles of Experimental Microsdosimetry," Radiat. Prot. Dosim., **61**, (1995) 297-308.

7. International Commission on Radiation Units and Measurements, "The Quality Factor in Radiation Protection," ICRU Publication 40, April 1986.

8. S. Gerdung, P. Pihet, J.E. Grindborg, H. Roos, U.J. Schrewe and H. Schuhmacher, "Operation and Application of Tissue Equivalent Proportional Counters," Radiat. Prot. Dosim., **61**, (1995) 381-404.

9. H. Schuhmacher, "Tissue Equivalent Proportional Counters in Radiation Protection Dosimetry: Expectations and Present State," Radiat. Prot. Dosim., **44**, (1992) 199-206.

10. A.J. Waker, "Microdosimetric Radiation Field Characterisation and Dosimetry in a Heavy Water Moderated Reactor Environment," Radiat. Prot. Dosim., **52**, (1994) 415-418.

11. J.C. Nunes, A.J. Waker and A. Arneja, "Neutron Spectrometry and Dosimetry in Specific Locations at Two CANDU Power Reactors," Radiat. Prot. Dosim., **63**, (1996) 87-104.

12. V. Michalik, F. Pernicka, F. Spurny and V.D. Nguyen, "Some Aspects of the Exposure of Aircraft Crew Members to Cosmic Radiation," Radiat. Prot. Dosim., **54**, (1994) 255-258.

13. L. Lindborg, J. Karlberg and T. Elfhag, "Legislation and Dose Equivalents aboard Domestic Flights in Sweden," Radiat. Prot. Dosim., **48**, (1993) 47-50.

14. V.D. Nguyen, P. Bouisset, G. Kerlau, N. Parmentier, Y.A. Akatov, V.V. Archangelsky, L.N. Smirenniy and M. Siegrist, "A New Experimental Approach in Real Time Determination of the Total Quality Factor in the Stratosphere," Radiat. Prot. Dosim., **48**, (1993) 41-46.

15. D. Regulla and J. David, "Measurements of Cosmic Radiation on Board Lufthansa Aircraft on the Major Intercontinental Flight Routes," Radiat. Prot. Dosim., **48**, (1993) 65-72.

16. H. Schuhmacher and U.J. Schrewe, "Dose Equivalent Measurements on Board Civil Aircraft," Physikalisch Technische Bundesanstalt, PTB-Bericht, PTB-N-13, Braunschweig, March 1993.

17. V.D. Nguyen, C. Luccioni and N. Parmentier, "Average Quality Factor and Dose Equivalent Meter Based on Microdosimetry Techniques," Radiat. Prot. Dosim., **10**, (1985) 277-282.

18. E.J. Waller and F.J. Lemay, , "Lead Lined REM Meter (LLRM) Calibration Study," SAIC Canada, presented to DREO, September 1997.

[19] J.K. Shultis and R.E. Faw, Radiation Shielding, Prentice Hall PTR, Upper Saddle River, NJ (1996).